

SCOPE-1: On-Orbit Surface Feature-Based Navigation and Timing Mission Overview

Paula Delfin, Lance Lui, Margaret Lambert, Dominic Nguyen, Meenakshi Kalinathabotla, Dylan McIntyre, Maximilian Riccioli, Riley Vazquez, Yan Zhe Wong, Yulia Meza, Brandon Jones, Renato Zanetti
 The University of Texas at Austin
 2617 Wichita Street, Austin, TX 78712; +1 (512) 471-7593
 paula.delfin@utexas.edu

ABSTRACT

The SpaceCraft for Optical-based Position Estimation-1 (SCOPE-1) is a 3U CubeSat developed by the Texas Spacecraft Laboratory (TSL) at The University of Texas at Austin to demonstrate near real-time Position, Navigation, and Timing (PNT) estimation primarily using optical detections of Earth’s islands and archipelagos. The mission adapts algorithms originally developed for lunar crater-based PNT and applies them to terrestrial features for validation in low Earth orbit (LEO). SCOPE-1 features an onboard system combining Mask R-CNN-based surface-feature detection, catalog-based feature identification, and an extended Kalman filter (EKF) to estimate position and timing in near real-time. The SCOPE-1 spacecraft will be built with primarily commercial off-the-shelf (COTS) components and will operate in LEO for one year following a planned 2027 launch. Additionally, the TSL is constructing an on-site ground station with UHF and S-Band capabilities to support in-house mission operations. This mission advances the technology readiness level (TRL) of the surface feature-based navigation algorithms and serves as a key step toward enabling autonomous navigation for future lunar and deep space missions. This paper presents an overview of the SCOPE-1 mission, including its objectives, concept of operations (ConOps), payload system, PNT algorithms, and spacecraft design.

INTRODUCTION

With renewed national and commercial interest in lunar and deep space exploration, there is an increasing demand for technologies that can support sustained, autonomous operations beyond Earth orbit. In particular, spacecraft operating in these regions will require reliable onboard navigation capabilities independent of traditional support infrastructure such as the Global Navigation Satellite System (GNSS) and the overtaxed Deep Space Network (DSN). Current methods for spacecraft navigation in lunar and deep-space environments rely primarily on ground-based tracking, inter-satellite communication, or legacy optical techniques, each with limitations in terms of autonomy, operational regimes they support, and hardware complexity. These constraints are particularly significant for CubeSats, which are expected to play a growing role in future lunar missions because of their accessibility and affordability. However, no current CubeSat platform provides an onboard, self-contained solution for near real-time PNT estimation using optical observations of central-body surface features. This absence highlights a critical gap in terrain-relative navigation capabilities for autonomous small spacecraft oper-

ations in support-denied environments such as cislunar space.

Several recent missions have demonstrated and evaluated other forms of autonomous navigation capabilities for CubeSats in the near-lunar environment and deep space. For example, CAPSTONE successfully demonstrated autonomous orbit estimation using two-way ranging with the Lunar Reconnaissance Orbiter (LRO) and a one-way uplink ranging navigation approach with NASA’s Deep Space Network.¹ Other missions have used optical navigation with horizon sensing or limb fitting, which support position and attitude estimation relative to celestial bodies.^{2,3} While these approaches have proven effective for their respective mission goals, they rely on different navigation principles —and in CAPSTONE’s case, require an external reference (e.g. another satellite) —than those used in surface feature-based approaches. Surface feature-based navigation enables PNT estimation by detecting and identifying specific terrain features, often using computer vision, without relying on external infrastructure. Despite growing interest in optical navigation, no CubeSat mission to date has performed fully autonomous onboard PNT estimation through surface feature detection and identification

with computer vision.

The SCOPE-1 mission aims to directly address this technological gap by flight-demonstrating a complete PNT estimation pipeline on board a 3U CubeSat using optical observations of Earth’s islands and archipelagos and GNSS-derived synthetic range measurements. The range measurements emulate those that can be produced during communication between the DSN and the spacecraft, and enable onboard clock bias and drift estimation.⁴ This differs from existing techniques that compute clock corrections by comparing the satellite clock to a highly precise solution on the ground. The system integrates three key algorithms: a Mask R-CNN-based model for surface feature detection, a catalog-matching process for surface feature identification and geolocation, and an EKF for fusing observations into near-real-time estimates of position and timing. These algorithms will be executed entirely on board the spacecraft, using primarily COTS hardware, within the strict size, power, and compute limitations imposed by the CubeSat form factor. A cutaway diagram of the SCOPE-1 CubeSat is shown in Figure 1. By adapting vision-based terrain-relative navigation techniques originally developed for crater-based lunar applications, SCOPE-1 aims to advance the TRL of these algorithms from TRL 4 to TRL 9. In doing so, the mission contributes to NASA’s Technology Taxonomy TX17.2.1 (Onboard Navigation Algorithms) and responds directly to NASA’s 2024 Civil Space Shortfalls #1557 and #1433, which call for autonomous PNT solutions for small spacecraft and in-orbit applications.^{5,6}

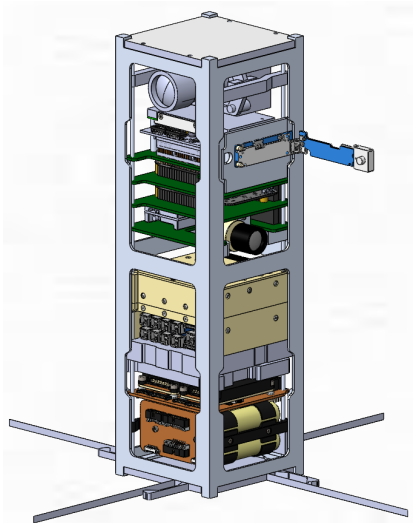


Figure 1: SCOPE-1 CAD

SCOPE-1 also supports next-generation infrastructure like NASA’s LunaNet, a scalable framework

of satellite nodes providing communication and navigation services.⁷ In LunaNet, some nodes provide communication services, while others enable navigation. To reduce ground support of the network, a subset of LunaNet nodes must use autonomous navigation and timing to support client PNT services. Optical navigation using crater-based techniques with infrequent ground contacts provides one approach to realize these capabilities.^{4,8} In traditional navigation beyond the near-Earth infrastructure, time estimation is enabled through ground-based orbit determination and clock estimation. This solution is then uploaded to the spacecraft. For SCOPE-1, this process is replaced with a GNSS-derived synthetic range observation. The filter measurement model includes correlation between timing and surface-feature localization errors, and periodic range measurements referenced to a different clock, in this case GNSS time, enable onboard timing estimation.⁴

This paper presents an overview of the SCOPE-1 mission, its technical design, and its relevance to future lunar and deep-space exploration. The Mission Objectives section outlines the mission’s goals and success criteria. The ConOps section outlines the planned operational timeline and imaging cadence during the one-year mission in LEO. The Vehicle Overview section describes the system architecture, breaking down the spacecraft into key subsystems, including payload components and ground support infrastructure. The Payload and PNT Algorithms section details the implementation of onboard image processing, feature identification, and EKF-based state estimation. The paper concludes with a discussion of the mission’s current status and planned future work.

MISSION OBJECTIVES

The primary goal of the SCOPE-1 mission is to demonstrate PNT estimation using optical detections of Earth’s islands and archipelagos and GNSS-derived synthetic range measurements. This mission will serve as a near-Earth demonstration of technology originally developed for operations near the Moon, with the intent of increasing the TRL of the PNT estimation algorithms for future near-lunar applications. To support this goal, the mission defines two tiers of success:

- **Minimum Success Criteria:** Successfully downlink a sufficient volume of images and ground-truth GNSS measurements to enable ground-based validation of the PNT algorithms.

- Full Success Criteria: Successfully execute the complete PNT pipeline on board the satellite in near-real-time, and downlink the position and timing results for ground-based validation.

Achieving a minimum level of success would raise the TRL of the PNT estimation algorithms from 4 to 8. Achieving full success will demonstrate that the system has achieved TRL 9 capability. The desired technical goals are:

1. Demonstrate on-orbit positioning using optical measurements of surface features
2. Demonstrate on-orbit timing using synthetic range measurements.

These goals are then decomposed into the following objectives that form the basis of the project requirements:

1. Estimate positioning in near-real-time, with less than 100 meters per axis error in situ using optical observations of primary-body surface features
2. Estimate timing in near-real-time, with less than 100 milliseconds error in situ using synthetic range observations.

These goals and objectives define the scope of the SCOPE-1 technology demonstration and provide a framework for assessing the system's readiness for operational deployment in similar support-denied environments.

CONCEPT OF OPERATIONS

SCOPE-1 was selected as a NASA CubeSat Launch Initiative (CSLI) mission and is currently awaiting assignment of a launch provider and date. This section provides a high-level description of the ConOps. This includes the sequence and timing of major events following the satellite's successful deployment into its operational orbit, as illustrated in Figure 2. While the ConOps is subject to refinement once launch details are finalized, the current version establishes a foundational understanding of the mission's phases, critical activities, and anticipated timelines, independent of launch-specific details.

Before deployment, the spacecraft will be placed inside a standard CubeSat deployer, such as a Poly Picosatellite Orbital Deployer (P-POD) or equivalent, which activates the onboard limit switches. During this time, the spacecraft will be disconnected from the power system and battery and will not be able to power on. In this state, the battery will be

charged to a level dependent on CubeSat storage duration prior to launch, and the UHF antenna on board the spacecraft will be in the stowed position. The mission timeline begins immediately after separation from the launch vehicle and deployment from the CubeSat deployer.

Shortly after ejection from the CubeSat deployer and release of the limit switches, the spacecraft's power system will be activated and begin supplying power to the other subsystems. The flight computer boots its operating system and begins the mission elapsed timer. After the flight computer completes its boot and establishes a connection with the Attitude Determination and Control System (ADCS), the detumble sequence will begin. After 45 minutes have elapsed, the UHF antenna will deploy, and the spacecraft will begin transmitting a health beacon every 15 seconds. The TSL will receive the satellite's TLE set, contingent on delivery from authorized space tracking entities, and begin the initial checkout by operator command. The satellite will first establish internal communication with the power, thermal, and communications subsystems. A test command will be sent, and logs of the respective subsystems will be returned to determine that all systems are operating without error and within predicted ranges. Then, the satellite will be given a command to execute an attitude maneuver to a particular direction vector. Results from this test and a log of the ADCS will be downlinked to confirm the system's integrity.

Following initial checkout, the satellite will enter Idle/Command Execution (I/CE) mode and listen for commands from the ground station. Next, the payload checkout is conducted by calibrating the imaging system and verifying that the inference pipeline is functional. Assuming at least one photo is taken during each pass, commands are sent to correct any issues detected in the images taken. During these passes, the imaging system's functionality and performance are verified, and necessary corrections are made to ensure that the satellite can successfully capture high-quality images for the intended experiment. The spacecraft is then ready to conduct the experiment and will remain in the I/CE state until a command is received from the ground station.

To initiate an experiment, the ground station will transmit a command containing specific experiment parameters to the spacecraft during a designated communication window. Following receipt of the command, the spacecraft will autonomously execute the experiment at a predetermined time and location. The duration of each experiment will vary depending on the quantity and frequency of image

❶	Launch
❷	Deployment from 3U dispenser
❸	Power On and Boot Up ($T+0$ sec)
❹	Detumble Begins (duration: 64 min; $T+30$ sec)
❺	Antenna Deployment ($T+45$ min) First Communication ($T+ \leq 1$ week) and Initial Checkout ($T+ \leq 1-2$ weeks)
❻	Payload Checkout and Camera Calibration ($T+ \leq 2-3$ weeks)
❼	Imaging Experiment (duration: 7-365 days)
❽	Mission End and Disposal (duration: <5 years)

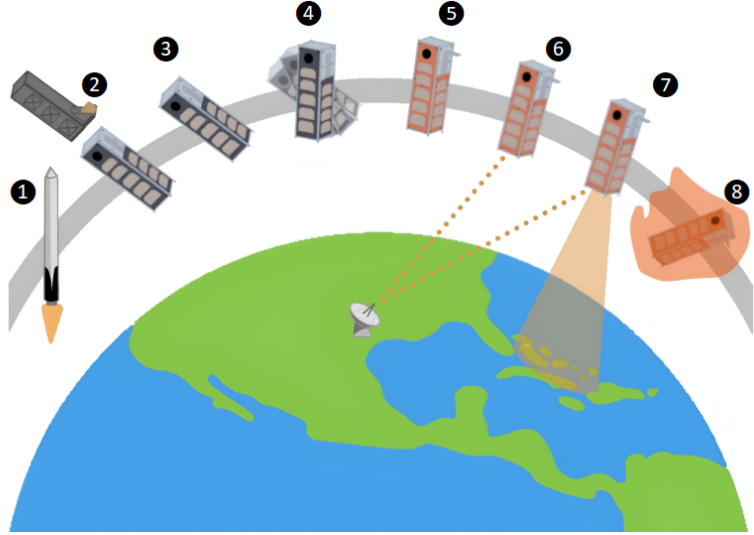


Figure 2: SCOPE-1 Concept of Operations

acquisitions dictated by the experiment command. The sequential stages of each experiment, along with their respective durations, are outlined below:

- **Payload System Initialization (~1 min):** The payload system will undergo a one-minute initialization process.
- **Achieve Nadir Pointing (~5 min):** The spacecraft will orient itself to achieve nadir pointing, a process lasting approximately five minutes.
- **Begin Recording Experiment Data:** The spacecraft will begin recording time-stamped attitude and GNSS data corresponding to the images being taken. The image capture sequence will be executed as defined by the specific parameters of the experiment command.
- **Run Inference and Compute PNT Estimates and Errors (~10 s per image):** For each captured image and corresponding time tag, the onboard payload computer will execute the inference algorithm and compute PNT estimates along with associated errors, requiring approximately ten seconds per image.
- **Save Results (1 s per image):** The computed results will be saved to onboard storage.

Although mission success only requires one demonstration of the PNT algorithm, multiple experiments may be conducted to collect additional

data. After all experimentation is finished and the mission is considered to be complete, the ground station will send a command to transition to the end-of-life operations. First, all power from the reaction wheels will be dissipated. Then the satellite will remain in the I/CE state until all remaining power is depleted. The spacecraft will naturally deorbit within 5 years following the Federal Communications Commission (FCC) regulation.⁹

VEHICLE OVERVIEW

SCOPE-1 is a 3U CubeSat equipped with an imager, dual radios, a GNSS receiver for ground truth, and dedicated computing for PNT inference. To reduce development costs and ensure reliability, the spacecraft primarily uses COTS components with proven flight heritage. Custom hardware is included to interface with non-standard components and will undergo equivalent qualification testing to ensure mission readiness. Table 1 outlines the high-level spacecraft specifications.

To facilitate the mission flow, the SCOPE-1 ConOps is realized in eight operational modes. Operational modes describe the state of spacecraft hardware and software. Automated triggers and commands prompt the transition between operational modes. Figure 3 depicts these states and transitions. Notably, two off-nominal states govern the satellite's response to errors: Low Power and Fail-Safe. The Low Power state is a general error mode activated upon detection of any onboard anomaly, including low power. In this state, only essential

functions continue, and non-essential activities are paused until the satellite returns to I/CE mode. A health beacon is transmitted to the ground station, and the ADCS optimizes the spacecraft's attitude for heating and charging. Importantly, interrupted or triggered non-essential functions are stored and will resume upon exiting Low Power mode. The Fail-Safe mode represents a minimum operation state, executing only a health beacon transmission and a system reboot under specific conditions. This mode also ensures compliance with FCC regulations by silencing the satellite after a prolonged loss of communication from the ground. Both Fail-Safe and Low Power modes are engineered to maintain a positive net power balance.

Table 1: Vehicle Specifications

Size	3U
Mass	3.53 kg
Battery Capacity	86 Wh
Energy Generation	1W Triple Junction Solar Cells (x22)
Compute	ARM Cortex A8 (x2) NVIDIA Carmel ARMv8.2 NVIDIA Volta GPU
Attitude Control	3-axis control via orthogonal reaction wheels
On Board GNC	Multi-frequency GNSS Receiver Star Tracker Sun Sensors (x6) Gyroscopes (x2)
Communication	Downlink: 435-438 MHz, 2400-2450 MHz Uplink: 435-438 MHz
Imaging	2592 X 1944 px 5 MP CMOS

SCOPE-1 employs a standard CubeSat design and mission organization, dividing its functionality into seven subsystems: Electrical Power System (EPS), Command and Data Handling (CDH), Communications (COM), Payload (PAY), Flight Dynamics System (FDS), Structure (STR), and Thermal Protection System (TPS). Each of these subsystems has its own unique hardware, software, and interfacing needs. The following subsections detail the components and specifications of each of these subsystems. Further details related to the payload system and algorithm implementation are provided separately in the Payload and PNT Algorithms section of this paper.

Electrical Power System

SCOPE-1 utilizes a COTS CubeSat power system with an integrated array conditioning unit and power distribution unit. The battery pack contains eight lithium-ion cells, totaling 86 Wh of capacity. The power system supplies the PC104 stack with regulated 12, 5, and 3.3 V across nine outputs. In orbit, the power system will be charged using 22 triple junction solar cells, each generating approximately 1 W of power.

Command and Data Handling

The CDH subsystem manages spacecraft command processing, data handling, and software execution. The subsystem employs a primary BeagleBone Black single-board computer, selected for its flexible input/output and flight heritage, with a secondary BeagleBone Black in the payload subsystem serving as a backup. The BeagleBone black utilizes a 1 GHz ARM Cortex A8 CPU and a NEON floating-point accelerator. The computer also features 512 MB of DDR3 RAM. Custom PC104-compliant printed circuit boards integrate both computers into the spacecraft bus. The flight software leverages NASA JPL's open-source F Prime framework, which uses a component-based architecture to manage mission-specific logic, device control, and hardware interfaces.¹⁰ Key components include a GNSS Module that handles measurements recorded by the GNSS Receiver and an FDS Manager Module that handles ground communication. There are three layers to the F Prime architecture: application, manager, and driver. The application layer handles the mission-specific logic. The manager layer handles device control, and the driver level is dedicated to specific hardware interfaces. The flight software is being developed in sections based on the needs for each subsystem and will be implemented at the driver level.

Communications

The COM subsystem enables command uplink, status downlink, and payload data transmission. The subsystem includes an Endurosat UHF transceiver with an omnidirectional antenna and an Endurosat S-band transmitter with a patch antenna. The UHF system operates at 435-438 MHz with a data rate of up to 19.2 kbps for command and status communication. The S-band system operates at 2400-2450 MHz with a data rate of up to 20 Mbps for payload data downlink. The UHF antenna deploys post-launch, while the S-band antenna is mounted

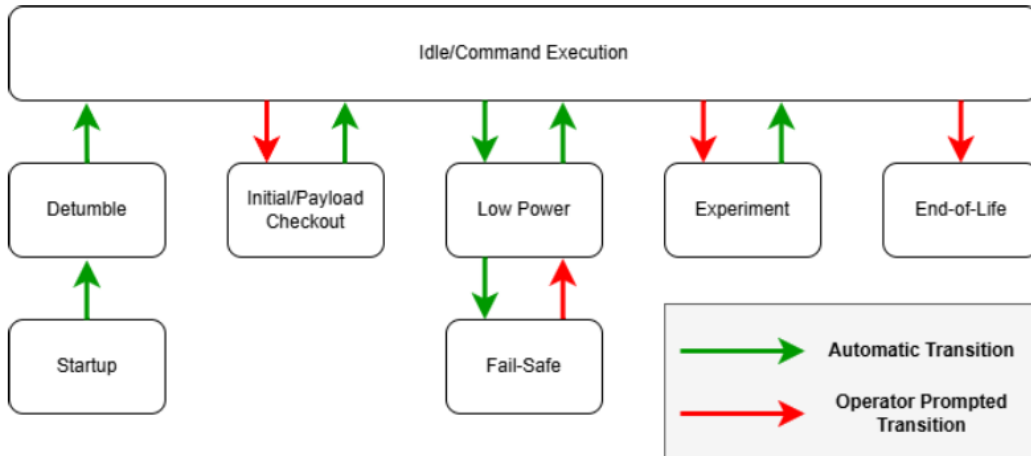


Figure 3: SCOPE-1 Operational Modes

on the spacecraft's +Z face. Both components are rated for amateur frequency bands.

Payload

The PAY subsystem integrates a Redwire SpectraCam high-resolution imager with the Jetson Xavier NX compute module. Images are captured at up to 10 Hz and processed using an optimized inference pipeline. The system supports a circular buffer for storing processed outputs, which include both annotated image snippets and state vector metadata. To manage thermal loads, the Jetson is thermally coupled to the spacecraft chassis using an aluminum heat bridge and passive fins. Thermal benchmarks confirmed > 5 minutes of continuous operation without throttling under nominal EPS settings. Power draw during inference peaks at approximately 11W, within system tolerances.

Flight Dynamics System

The planned near-circular orbit of SCOPE-1 must meet the FCC's five-year deorbit requirement and a mission duration of at least one year. The acceptable altitude range is determined through MATLAB simulations employing the System Tool Kit (STK) Orbit Lifetime tool, accounting for the Earth's J_2 perturbation, solar radiation pressure, and atmospheric drag (Jacchia 1970 model).¹¹ The operational altitude range extends from 460 km to 510 km. The inclination of the selected orbit ensures consistent data downlink visibility with the ground station located at The University of Texas at Austin. The suitable inclination range is from

30.28° to 149.72°, and is determined by the latitude of Austin, TX.

The ADCS for SCOPE-1 utilizes a CubeSpace CubeStar Gen 2 star tracker, ten coarse sun sensors, and a CubeSpace CubeTorquer magnetometer for attitude determination. These sensors provide an absolute attitude knowledge error of less than 0.06°. The position of the star tracker on the satellite body is verified using STK simulations to ensure the Sun and Moon remain at 90° angle or greater from its boresight. The GNSS receiver selected for SCOPE-1 is the NovAtel OEM7600H, chosen for its high velocity limit (600 m/s), multi-frequency capability, and compact size.

The ADCS utilizes the CubeSpace CubeTorquer magnetorquer and three CubeSpace CubeWheel reaction wheels as actuators. Immediately after launch, the magnetorquer detumbles the satellite, achieving Y-Thomson spin stabilization.¹² Due to the satellite's presence in a high magnetic field environment characteristic of LEO, the magnetorquer also performs momentum dumping to manage reaction wheel desaturation. Following stabilization, the reaction wheels provide minor attitude corrections to maintain the Redwire SpectraCAM's nadir-pointing orientation. Each reaction wheel aligns along one of the principal axes (x, y, or z) to ensure precise attitude control in all directions.

Structure

The primary structural framework of SCOPE-1 utilizes the EnduroSat 3U CubeSat Structure, constructed primarily from aluminum alloy 6082. Figure 4 presents an exploded view of the spacecraft,

illustrating the placement of the structural elements and major components, as well as the body-fixed reference coordinate axes to assist in interpreting component orientations. The chassis incorporates PC104-compliant threaded rods along the z-axis, streamlining component integration by reducing the number of required fasteners. The external surfaces of the chassis are hard-anodized for durability and environmental compatibility. The SCOPE-1 STR team custom-designs and fabricates additional structural elements, including an external mounting bracket for the magnetometer and internal brackets for the flight camera, star tracker, and GNSS antenna. All custom brackets use machined aluminum alloy 6061 and undergo anodization.

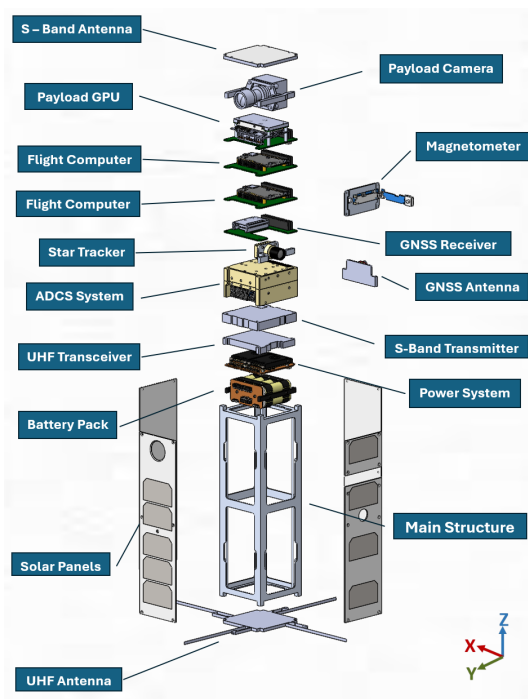


Figure 4: SCOPE-1 Exploded View

The payload camera serves as the primary reference for the orientation of SCOPE-1's sensor components and maintains a nominal nadir-pointing alignment along the +Y face. The GNSS antenna adopts a zenith-pointing configuration along the -Y face, while the magnetometer and star tracker are oriented 90 degrees from nadir in the -X direction. The S-band antenna is mounted at the top of the 3U structure on the +Z face, and the UHF antenna is attached to the bottom of the structure on the -Z face. The primary power of the spacecraft is generated by 22 solar cells mounted across the lateral $\pm X$ and $\pm Y$ faces of the chassis.

Thermal Protection System

The thermal protection subsystem consists of sixteen Texas Instruments thermistors with twelve external placements and four internal placements to monitor the temperature of the satellite in locations of interest. Areas subject to extreme temperature changes include external-facing electronics such as the GNSS antenna, the magnetorquer, the camera, and antennas on the Z faces of the satellite. Other locations of interest include internal components with high heat loads, such as the battery and power distribution, flight computer, ADCS, and the camera. The thermal protection subsystem assigns a thermistor to all the components listed above. The distribution of the remaining thermistors concentrates on solar panels and the exterior walls of the satellite.

Ground Station

The TSL is currently building an on-site ground station to support the SCOPE-1 mission operations. The ground station will utilize COTS components to enable both S-band and UHF communication with the satellite. The ground station incorporates RF Hamdesign hardware alongside custom REMOS components. A REMOS expedite modem and sequencer manage the ground station, automating satellite tracking, antenna control, modulation/demodulation, pass scheduling, and data management. UHF communication employs Yagi antennas, while S-band operations utilize a 3-meter dish from RF Hamdesign. All components have been delivered to the TSL, and members are working on integrating the system into the building's facilities.

PAYLOAD AND PNT ALGORITHMS

The onboard payload system is designed to enable autonomous PNT estimation for small satellites in LEO primarily using terrestrial surface features. This system provides near real-time localization by detecting islands and archipelagos in nadir-pointing imagery. These features are matched with reference data to estimate the spacecraft's location and velocity. To estimate time, SCOPE-1 uses synthetic range measurements computed from GNSS-derived position estimates that are precisely time-tagged. The goal is to reduce the dependence on near-Earth and ground-based navigation infrastructure, enabling greater autonomy. Note that the onboard PNT algorithms do not use the GNSS pseudorange measurements to directly estimate the clock bias and drift. Instead, the GNSS-determined point

solution is used to create a synthetic range measurement relative to a known location with a precise time tag. This time tag corresponds to a known transmission time from a ground-based signal, establishing an external reference that enables onboard clock bias estimation.

This approach adapts legacy Crater-based Navigation and Timing (CNT) technology, originally developed for lunar missions, to Earth environments.^{4,8} Algorithms downstream of the detector (identification, the EKF, etc.) are the same as the CNT system. CNT was initially developed for lunar spacecraft to localize in GNSS-denied scenarios using crater detections and surface maps. Lunar craters, being symmetric and consistent, provided ideal features for localization. However, Earth’s irregular island shapes, lighting variability, and proximity to landmasses pose new challenges. The CNT framework was adopted at the TSL by redesigning its architecture and tailoring the detection algorithms to support the identification of islands and archipelagos in Earth imagery.

As shown in Figure 5, the payload system implements a multi-stage pipeline to process nadir-pointing imagery and support onboard navigation. Captured images are passed to a convolutional neural network running on the NVIDIA Jetson Xavier NX that performs island segmentation by regressing pixel-wise masks. Island centroids are calculated from these masks, and both the raw segmentation output and centroid data are stored locally. An example of the computer vision model creating island masks, performing instance segmentation, and generating centroids is shown in Figure 6 for the Cayo Campos island located in the Caribbean.

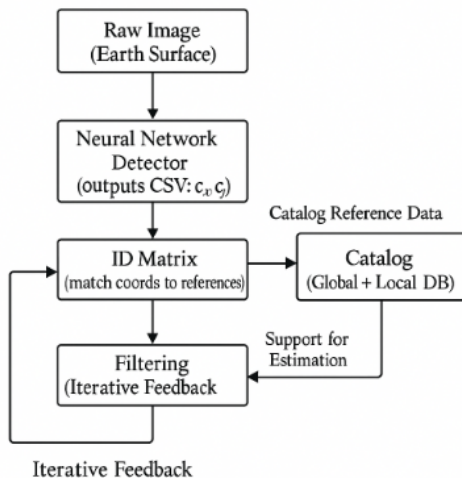


Figure 5: Estimation Pipeline

The inference results can then be used to perform identification against a reference terrain catalog on board. The set of matched island features serves as the basis for measurement updates within a navigation filter, which estimates the spacecraft’s position, velocity, and clock bias over time. This filtering framework supports recursive estimation, allowing the system to maintain state awareness across successive frames while accounting for measurement uncertainty and dynamic model propagation. In this context, the neural network detector outputs the pixel coordinates c_x and c_y that represent the centroid locations of detected island features in image space.

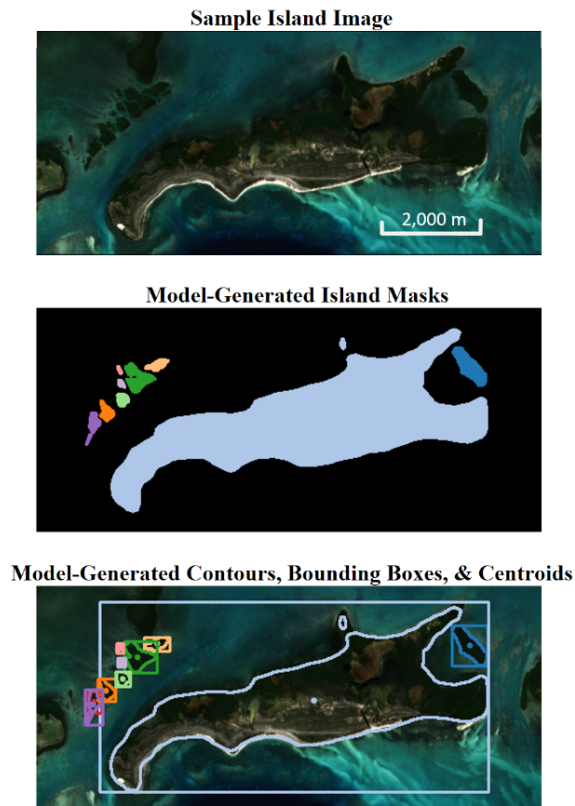


Figure 6: Cayo Campos Example

The neural network utilizes a convolutional architecture derived from Faster R-CNN to detect islands of varying sizes, shapes, and edge definitions. Over approximately 10,000 satellite images were retrieved from NASA Global Imagery Browse Services (GIBS), Sentinel HUB, Google Earth Engine, STACStack with catalogs from STAC Index, and Copernicus Dataspace Ecosystem to capture diverse conditions, including cloud occlusion, glare, and adjacent landmasses.^{13–18}

The viability of island-based navigation for orbital PNT estimation was assessed through high-

fidelity orbital image simulation, incorporating altitude and lighting conditions. Details of the simulation setup and feature visibility analysis are presented in the paper by Agrawal and Jones, which confirmed sufficient island detection coverage across typical LEO passes.¹⁹

The analysis focused on two primary constraints: the minimum resolvable island size necessary for reliable detection and the spatial extent of the image footprint to ensure that multiple reference features would be visible per frame. We selected the camera’s field-of-view so that each frame includes multiple, spatially separated island features, thereby increasing the number of simultaneous measurements available for the navigation filter. This increases the number of independent measurements available to the navigation filter, which in turn reduces the time required for the filter to converge on an accurate position solution.

To support accurate navigation estimation under diverse imaging conditions, the camera exposure may be set anywhere from 0.1 ms to 5000 ms, enabling robust captures in high-contrast scenes such as sun-glint, cloud cover, and terrain shadows. In operation, the payload acquires imagery at 10 Hz, while the onboard PNT pipeline aims to execute updates at 0.1 Hz (once every 10 s). Capturing at 10 Hz provides temporal oversampling within each PNT update interval. By capturing imagery at 10 Hz, the system provides multiple frames within each PNT update window, increasing data redundancy and offering more opportunities to detect usable landmark features. External compute and buffering subsystems handle the increased data flow by running every captured frame through the segmentation network and queuing the results. The navigation filter then performs its measurement update using the most recent centroids (c_x, c_y) only once per 10 s interval. This approach balances high-rate imaging, which improves redundancy, with the navigation filter’s practical update interval, all while remaining within the spacecraft’s power, thermal, and processing constraints.

The combined effect of these imaging system capabilities ensures that the payload satisfies the core technical goals and objectives of the mission. The system captures and processes imagery at 10 Hz to provide temporal oversampling for the PNT pipeline, which executes updates at 0.1 Hz. The high-rate imaging cadence improves data quality and redundancy, while adjustable exposure ensures consistent detection of island features under variable lighting and viewing conditions. Together, these attributes support autonomous localization in Earth-

observing environments without continuous reliance on GNSS coverage, while operating within spacecraft resource constraints. References to detailed methodology and performance results can be found in Agrawal and Jones.¹⁹

CURRENT STATUS AND FUTURE WORK

SCOPE-1 successfully completed its critical design review on January 13, 2025, and is currently preparing for both the Pre-Procurement Readiness Review and the System Integration Review, to be conducted with CSLI and Small Spacecraft Technology Program (SSTP), respectively, in either Q3 or Q4 of 2025. Subsystem analyses and budgets are nearly finalized, with only minor adjustments remaining. Most components have been ordered, and component-level verification testing has begun. However, supply chain disruptions and extended manufacturer lead times have contributed to delays in acquisition. Additionally, recent fluctuations in tariff rates for components from non-US vendors have introduced uncertainty in cost projections. These predicted costs are currently within the project’s financial budget margin.

Immediate action items include the development of a FlatSat for subsystem and system-level testing, and maturing both our mission and payload flight software. In addition, the TSL is in communication with the National Oceanic and Atmospheric Administration (NOAA) Commercial Remote Sensing Regulatory Affairs (CRSRA) division to obtain a remote sensing license. Once the remote sensing license is obtained, the TSL will begin coordinating with the International Amateur Radio Union (IARU) to receive an amateur radio frequency allocation.

ACKNOWLEDGMENTS

This material is based upon work supported by NASA under award No. 80NSSC20M0087. Any opinions, findings, and conclusions or recommendations expressed in this material are those of the authors and do not necessarily reflect the views of the National Aeronautics and Space Administration.

The authors would like to thank NASA’s Small Spacecraft Technology Program and the CubeSat Launch Initiative for their guidance and support as part of this project. Furthermore, the authors thank the graduate research assistants who contributed to this work, including Anand Agrawal and Andrea Rigato, as well as the broader team at the TSL for their hard work and dedication. In particular,

we would like to recognize Srinithya Challa, Saanvi Ahota, Vignesh Winner, Avi Singh, William Zhang, Aditi Palavalli, Aditya Gandhi, Sairamana Sivakumar, Runtian Du, Ethan Snider, Sophia Gallo, Orhan Oconer, and Tori Hassmann for their efforts in advancing the SCOPE-1 mission.

References

- [1] T. Gardner, C. B., J. Parker, A. Forsman, E. Kayser, M. Thompson, C. Ott, L. DeMoudt, M. Caudill, M. Bolliger, A. Kam, K. Thompson, R. Rogers, H. Umansky, B. Bryant, and T. Svitek, “Capstone: A summary of a highly successful mission in the cislunar environment,” in *2023 Small Satellite Conference*, 2023, pp. SSC23-I-04.
- [2] T. Nguyen, K. Cahoy, and A. Marinan, “Attitude determination for small satellites with infrared earth horizon sensors,” *Journal of Spacecraft and Rockets*, vol. 55, no. 6, pp. 1466–1475, 2018. [Online]. Available: <https://doi.org/10.2514/1.A34010>
- [3] A. J. Liounis and K. Getzandanner, “Operational performance of limb-based navigation from osiris-rex at bennu,” in *3rd Space Imaging Workshop*, 2022. [Online]. Available: <https://ntrs.nasa.gov/citations/20220008145>
- [4] F. D’Onofrio and R. Zanetti, “Novel approach to autonomous lunar localization and timing,” in *Journal of Guidance, Control, and Dynamics*, vol. 47, 2023, pp. 36–48. [Online]. Available: <https://doi.org/10.2514/1.G007613>
- [5] NASA, “Civil Space Shortfall Ranking,” <https://www.nasa.gov/wp-content/uploads/2024/07/civil-space-shortfall-ranking-july-2024.pdf?emrc=6841c6c6db563>, 2024, accessed: 2025-06-01.
- [6] —, “2020 NASA Taxology Taxonomy,” <https://ntrs.nasa.gov/citations/20190032038>, 2019, accessed: 2025-06-01.
- [7] D. J. Israel, K. D. Mauldin, C. J. Roberts, J. W. Mitchell, A. A. Pulkkinen, L. V. D. Cooper, M. A. Johnson, S. D. Christe, and C. J. Gramling, “Lunanet: a flexible and extensible lunar exploration communications and navigation infrastructure,” in *2020 IEEE Aerospace Conference*, 2020, pp. 1–14.
- [8] Z. R. McLaughlin, R. E. Gold, S. G. Catalan, B. A. Jones, and R. Zanetti, “Crater navigation and timing for autonomous lunar orbital operations in small satellites,” in *Proceedings of the 44th Annual American Astronautical Society Guidance, Navigation, and Control Conference, 2022*, M. Sandnas and D. B. Spencer, Eds. Cham: Springer International Publishing, 2024, pp. 155–171.
- [9] Federal Communications Commission, “Space Innovation IB Docket No. 22-271 Mitigation of Orbital Debris in the New Space Age IB Docket No. 18-313,” <https://docs.fcc.gov/public/attachments/FCC-22-74A1.pdf>, 2022, accessed: 2025-06-01.
- [10] NASA Jet Propulsion Laboratory, “F” User Manual,” <https://fprime.jpl.nasa.gov/latest/docs/user-manual/>, 2024, accessed: 2025-06-01.
- [11] L. G. Jacchia, “Revised static models of the thermosphere and exosphere with empirical temperature profiles,” in *SAO Special Report No.332*, 1971.
- [12] W. T. Thomson., “Spin stabilization of attitude against gravity torque,” *Journal of Astronautical Science*, vol. 9, no. 1, pp. 31–33, 1962.
- [13] NASA Earthdata, “Global Imagery Brows Services (GIBS) APIs,” <https://www.earthdata.nasa.gov/engage/open-data-services-software/earthdata-developer-portal/gibs-api>, accessed: 2025-06-01.
- [14] Sinergise Solutions d.o.o., “Sentinel Hub,” <https://www.sentinel-hub.com/>, accessed: 2025-06-01.
- [15] Google LLC, “Google Earth Engine,” <https://earthengine.google.com/>, accessed: 2025-06-01.
- [16] SpatioTemporal Asset Catalog (STAC) Initiative, “STACStack: Tools and Servers for STAC Catalogs,” <https://stacstack.org/>, 2024, accessed: 2025-06-01.
- [17] —, “STAC Index: Centralized STAC Catalog Service,” <https://stacindex.org/>, 2024, accessed: 2025-06-01.
- [18] Copernicus Data Space Ecosystem, “Copernicus Data Space Ecosystem,” <https://dataspace.copernicus.eu/>, 2024, accessed: 2025-06-01.

- [19] S. A. Agrawal and B. A. Jones, “Satellite navigation with Earth islands for SCOPE-1,” in *2025 Small Satellite Conference*, Salt Lake City, UT, August 2025, pp. SSC25-P1–38.